

Evidence for the Supergene Origin of Alunite in Sediment-Hosted Micron Gold Deposits, Nevada

GREG B. AREHART, STEPHEN E. KESLER, JAMES R. O'NEIL,

Department of Geological Sciences, University of Michigan, Ann Arbor, Michigan 48109-1063

AND K. A. FOLAND

Department of Geological Sciences, Ohio State University, Columbus, Ohio 43210-1398

Abstract

On the basis of textural features and spatial distributions, both supergene and hypogene origins have been proposed for alunite in sediment-hosted micron gold deposits. If alunite is indeed primary, its presence provides important constraints on the chemistry of the ore fluid. Thus, determination of the genesis of alunite is critical to the understanding of the geologic history of these ore deposits.

At the Post deposit in Nevada K/Ar ages of alunite are much younger than the age of mineralization. Sulfur isotope compositions of alunite from several sediment-hosted micron gold deposits are virtually identical to those of sulfides, suggesting that alunite sulfur came from quantitative (closed-system) oxidation of primary sulfide minerals during weathering. Sulfur and oxygen isotope compositions of barite are markedly different from those of alunite. The oxygen and hydrogen isotope compositions of alunite fall in the supergene alunite fields; data for cogenetic kaolinite fall on the kaolinite line, whereas those for hypogene kaolinite do not. From all available petrographic and geochemical data, it would appear that alunite in the micron gold deposits of Nevada is entirely of secondary supergene origin.

Introduction

SEDIMENT-HOSTED micron gold deposits, located primarily in the eastern part of the Basin and Range province of western North America (Fig. 1), are currently the major source of gold in the United States. Alunite is common in these deposits and has been interpreted by some as a primary hypogene mineral associated in time with gold mineralization (e.g., Radtke, 1985; Ilchik, 1990). If alunite is indeed hypogene and related to gold mineralization, it could provide important constraints on the oxidation state and pH of sediment-hosted micron gold ore fluids. Such constraints significantly affect genetic and exploration models, particularly with regard to alteration assemblages as guides to ore. Therefore, it is imperative to make a critical assessment of the paragenetic relations of alunite in these important deposits.

Sediment-hosted gold deposits are localized predominantly within silty carbonate rocks of the lower to mid-Paleozoic shelf sequence that was deposited on the edge of the Precambrian craton. Gold mineralization comprises disseminated, stratiform replacements in these rocks and is associated with iron and arsenic sulfides, stibnite, barite, and hypogene kaolinite (Bagby and Berger, 1985; Bonham, 1985; Tooker, 1985). In some deposits minor but significant amounts of ore are found in igneous host rocks. Arsenic, the element most closely associated with gold mineralization, occurs most commonly within

arsenian pyrite and/or marcasite (Wells and Mullins, 1973; Radtke, 1985). Structural control of ore deposition is common, particularly on a local scale.

Alteration processes associated with these deposits include decarbonatization, silicification (jasperoid formation), argillization, and sulfidation, all of which are controlled by structure and stratigraphy (Radtke, 1985; Bakken and Einaudi, 1986; Hofstra et al., 1990). Detailed work at Carlin by Bakken and Einaudi (1986) documented various degrees of coupled decarbonatization and silicification within stratigraphic units ranging from "recrystallized calcite" farthest from ore through "moderate silicification" to "complete silicification" as fluid conduits are approached. Gold mineralization is highest grade in areas of incipient to moderate silicification. Decarbonatization is in large part preore and may have facilitated fluid flow by increasing porosity and permeability. Silicification also is in part preore, and jasperoids completely unrelated to ore are known (Northrop et al., 1987). Sulfidation as an important depositional mechanism has been proposed, based on work done in the Jerritt Canyon district (Hofstra et al., 1990). The latest alteration produces kaolinite, which grades outward into kaolinite-sericite. The kaolinite-only zone is primarily in feeder structures and areas of intense alteration adjacent to those structures (Kuehn and Rose, 1987; Arehart et al., 1989). Farthest from fluid conduits, no hydrothermal phyllosilicates were generated; however, primary

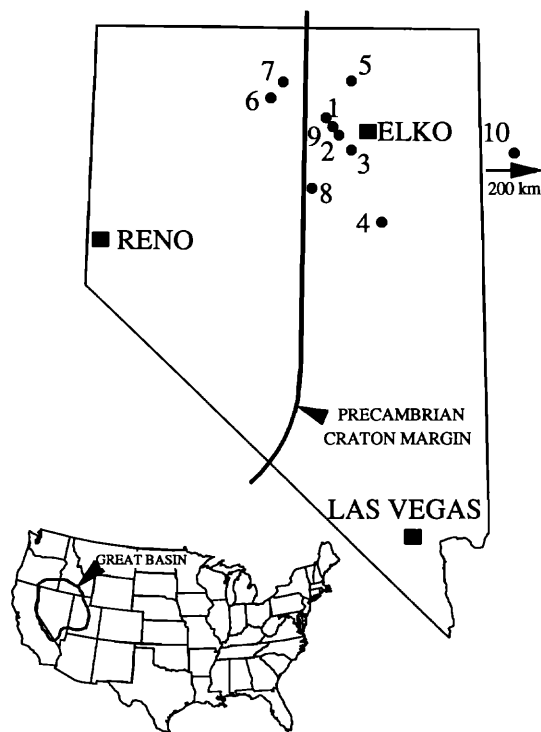


FIG. 1. Location map for major sediment-hosted micron gold deposits. Deposits included in this study are Post (1), Gold Quarry (2), Rain (3), and Alligator Ridge (4). Other major deposits include Jerritt Canyon (5), Getchell (6), Chimney Creek (7), Cortez (8), Carlin (9), and Mercur (10).

diagenetic and detrital kaolinite and muscovite are present in the rock.

Alunite can form under highly acidic and oxidizing conditions by several distinctly different processes. There has been some confusion in the literature regarding the terminology applied to alunite of these varying origins. Rye et al. (1991) have recently discussed the systematics of alunite formation, and their terminology will be used in this paper. Magmatic hydrothermal alunite forms where intrusion-driven hydrothermal systems contain significant magmatic components in the hydrothermal fluids (Rye et al., 1991). Alunite also may precipitate directly from the vapor phase in a magmatic steam environment, though such occurrences are rare (Cunningham et al., 1985). Steam-heated alunite may be generated in geothermal systems after oxidation of ascending H_2S gas to H_2SO_4 at or above the water table. The term "primary supergene" (e.g., Hayba et al., 1986) also has been applied to alunite of this origin. Supergene alunite (also termed "secondary supergene" by Hayba et al., 1986) forms in a low-temperature weathering environment from surficial (atmospheric) oxidation of primary sulfides.

Although these environments might be distinguished by their geologic characteristics, alunite in sediment-hosted micron gold deposits has been found only in near-surface exposures where surficial weathering has obscured these critical relations. Presumed primary hypogene oxidation has been overprinted nearly everywhere by secondary supergene oxidation, and it is difficult to separate the two events solely on the basis of field observations. Proponents of hypogene oxidation suggest that a structurally controlled oxidation event occurred late in the history of ore deposition (Radtke, 1985; Rye, 1985; Ilchik, 1990). Such interpretations are based in part on the presence of barite \pm alunite veins which are reported to pinch out with depth at the oxidized-reduced rock interface. While this pinching out may be the case for some deposits, it is not at Post, where vein barite persists to the deepest levels drilled thus far (>700 m). This vein barite is distinct from bedded and disseminated barite, which is Paleozoic in age and syngene in origin based upon sulfur isotope analysis (Ilchik, 1990; G. B. Arehart, unpub. data). In addition, Radtke (1985) and Ilchik (1990) suggest that hydrothermal silica was introduced during the oxidation event either by ore fluids or by the alteration of illite to kaolinite. At Carlin, silica flooding is reported to encase oxidized pyrite (Radtke, 1985). Field relations in which oxidized rocks underlie reduced rocks, such as at Alligator Ridge, have been interpreted as hypogene ascending oxidation (Ilchik, 1990).

Field, petrographic, and stable and radiogenic isotope measurements of sediment-hosted micron gold alunite were made in order to ascertain its origin. Unequivocal evidence for a secondary supergene origin of such alunite is provided by K/Ar dates that are distinctly younger than the age(s) of mineralization. Strong supporting evidence is provided by stable isotope systematics of alunite relative to those of coexisting sulfides, other sulfates, and kaolinite.

Textures and Mineral Associations of Alunite

At both the Rain and Gold Quarry deposits, alunite forms massive veins and replacement(?) pods in ore zones (Fig. 2A). These alunite veins are essentially monomineralic, with only traces of sericite, kaolinite, and quartz. Individual alunite crystals are commonly only a few micrometers in diameter and may be anhedral or euhedral. At Alligator Ridge, alunite occurs with barite in veins crosscutting quartz-kaolinite-(oxidized) stibnite veins and as massive veins cutting brecciated rock (Ilchik, 1990). Vein barite is usually overgrown by alunite, which locally is cut by jarosite. At Post, alunite forms earthy-pink to creamy-brown fracture fillings and is associated with jarosite, kaolinite, crandallite $[CaAl_3(PO_4)_2(OH) \cdot H_2O]$, pharmacosiderite $[Fe_3(AsO_4)_2(OH)_3 \cdot 5H_2O]$, symplectite $[Fe_3(AsO_4)_2 \cdot 8H_2O]$, stibiconite $[Sb_3O_6(OH)]$, and

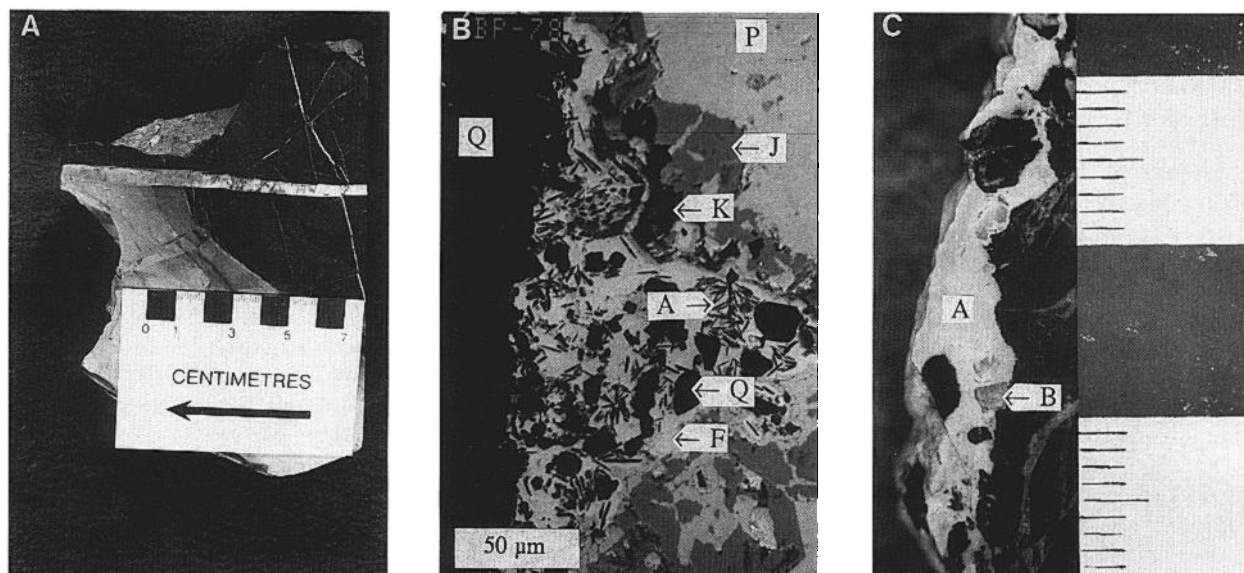


FIG. 2. A. Hand specimen of an alunite vein from the Gold Quarry deposit cutting both oxidized and reduced rock. This vein is essentially pure alunite, with only traces of illite and quartz. B. SEM backscattered image of a multiminerall breccia vein filling from the Post pit. Q = quartz, J = jarosite, K = kaolinite, A = alunite, F = Fe oxides, P = pharmacosiderite $[\text{Fe}_3(\text{AsO}_4)_2(\text{OH})_2 \cdot 5\text{H}_2\text{O}]$. C. Hand specimen of an alunite-bearing vein from the Post deposit showing the intergrowth of alunite (A) and barite (B). Alunite, $\delta^{34}\text{S} = 9.4$ per mil; barite, $\delta^{34}\text{S} = 27$ per mil. Tick marks on scale are 1 mm apart.

iron oxides, all of which commonly form in supergene environments (Fig. 2B). In contrast to paragenetic relations at Alligator Ridge, alunite at both Post and Mercur cuts or is present as overgrowths on jarosite (Jewell and Parry, 1987). There is no evidence that alunite was cogenetic with pyrite in any of these deposits, and alunite veins cut pyrite-bearing rock (Fig. 2A). One of the major arguments presented for a hypogene origin for alunite in sediment-hosted micron gold deposits is the presence of coexisting (presumed cogenetic) barite and alunite. Although barite may be a constituent of the same veins, it is usually coarsely crystalline, tabular, and clear, in contrast to the fine-grained earthy alunite (Fig. 2C). Where observed, barite always is paragenetically earlier than alunite. At the Post deposit, such barite is relatively common at depth as a late hydrothermal mineral to far below the oxide zone where alunite is absent.

Analytical Techniques

Alunite was separated by handpicking followed by treatment in HF to remove silicate contaminants (mostly quartz and kaolinite). For oxygen and sulfur isotope analyses, alunite was dissolved in 7.5 N NaOH followed by reprecipitation as BaSO_4 ; this procedure does not affect the isotopic composition of either O or S in sulfate (Lloyd, 1968; Chiba et al., 1981). Kaolinite, barite, and sulfides were either handpicked or sampled using a diamond bit on a dental drill. Scanning electron microscopy was done in

the University of Michigan electron microbeam analysis laboratory utilizing a Hitachi S-570 scanning electron microscope in backscattered electron and secondary electron modes.

All extractions and stable isotope measurements were done in the stable isotope laboratory at the University of Michigan. Sulfate oxygen extractions were done in a conventional fluorination line using BrF_5 ; $\delta^{18}\text{O}$ values were corrected utilizing BaSO_4 internal standards of known isotopic composition. Bulk alunite oxygen extractions were done by both conventional and laser-assisted fluorination (Sharp, 1990); internal standards were used for correction for incomplete reaction of the sulfate. We did not analyze hydroxyl oxygen separately. Hydrogen extractions from alunite and kaolinite were performed by the Zn-reduction method (Coleman et al., 1982; T. W. Venneman and J. R. O'Neil, in prep.). Both δD and $\delta^{18}\text{O}$ were measured on a Finnigan MAT delta-S mass spectrometer. Overall precision is better than ± 0.2 per mil for $\delta^{18}\text{O}$ and ± 1 per mil for δD . Sulfur extractions were done by standard techniques using Cu_2O (e.g., Robinson and Kusakabe, 1975) and isotopic ratios were measured on a VG-602 mass spectrometer. Precision of these analyses is ± 0.15 per mil.

Age determinations were made in the K/Ar laboratory at the Ohio State University. Potassium measurements were done in an IL 443 flame photometer utilizing an Li internal standard. Sample fusions were accomplished by induction heating, and argon mea-

surements were performed by isotope dilution using a Nuclide SGA-6-60 mass spectrometer operated in the static mode.

Age of Alunite

The age of alunite from the Post, Gold Quarry, and Rain deposits (Table 1) was determined in this study by conventional K/Ar analyses. Brown and pink alunite from Post are 8.6 ± 0.2 and 9.5 ± 0.2 Ma, respectively. Ages of 18.8 ± 0.3 and 20.0 ± 0.3 Ma were obtained for vein and pod alunite from two locations at Rain. Massive alunite from Gold Quarry is 25.9 ± 0.6 Ma. Four alunite samples from Alligator Ridge, reported by Ilchik (1990), have K/Ar ages which range from 10.9 ± 0.5 to 12.4 ± 0.5 Ma.

The ages of alunite samples from individual deposits are in reasonably good agreement with only limited dispersion. An age of 10.4 Ma for secondary supergene alunite from Goldfield, Nevada, agrees with the K/Ar ages of pre- and post-supergene vol-

canic events determined by Ashley and Silberman (1976). K/Ar ages of supergene alunite from Australia determined by Bird et al. (1990) also are geologically reasonable. Thus, it is inferred that the ages given above accurately represent the time of alunite formation.

The K/Ar ages for alunite at Post do not agree with ages for hypogene mineralization. K/Ar, $^{40}\text{Ar}/^{39}\text{Ar}$, and fission-track ages suggest mineralization at the Post deposit is about 110 Ma (Arehart et al., 1989). One well-constrained dike that cuts ore has been dated at 39 Ma. Zircon and apatite fission-track ages on this postore dike are concordant with those inferred from $^{40}\text{Ar}/^{39}\text{Ar}$ incremental-heating plateaus (G. B. Arehart, unpub. data). There is no evidence of any reheating above the closure temperatures for these minerals ($\sim 100^\circ\text{C}$ for apatite, $\sim 200^\circ\text{C}$ for zircon; Naeser, 1979). In marked contrast to the age of mineralization, alunite from the Post deposit ranges in age from 8.6 to 9.5 Ma. No reliable ages are available for the mineralization at other sediment-hosted micron gold deposits; reported ages range from 35 to 121 Ma, but none of the samples which were dated are well constrained to be related to mineralization. However, all published estimates of mineralization age (except the ages of alunite itself) significantly exceed the alunite ages.

TABLE 1. K and Ar Analytical Data and Calculated Ages for Alunite Samples from Nevada Sediment-Hosted Micron Gold Deposits

Sample ¹	K (wt %)	$^{40}\text{Ar}_{\text{rad}}$ (10^{-10} mole/g)	$\frac{^{40}\text{Ar}_{\text{rad}}}{^{40}\text{Ar}_{\text{total}}}$	Calculated age ² (Ma)
GQ-5280	6.15	2.747	0.651	
	6.20	2.823	0.623	
	6.19			
	6.13			
	6.14			
Average	6.16	2.785		25.9 ± 0.6
9834A	9.27	3.043	0.212	
	9.27	3.040	0.192	
Average	9.27	3.042		18.8 ± 0.2
9835A	9.21	3.224	0.506	
	9.21	3.206	0.552	
	9.21			
Average	9.21	3.215		20.0 ± 0.2
BP-79P	9.05	1.501	0.800	
	9.21	1.522	0.727	
	9.15			
Average	9.14	1.512		9.5 ± 0.2
BP-79B	8.95	1.359	0.746	
	8.98	1.321	0.691	
	8.97			
Average	8.97	1.340		8.6 ± 0.2

¹ Samples: GQ-5280, thick monomineralic alunite vein, Gold Quarry deposit; 9834A, monomineralic pod of alunite in limestone, Rain deposit; 9835A, alunite-kaolinite vein, Rain deposit; BP-79P, pink alunite from fractures in silicified rock, Post deposit; BP-79B, brown alunite overgrowing jarosite in veins, Post deposit
² Constants used: $^{40}\text{K} = 1.167 \times 10^{-2}$ atom percent of total K; $(^{40}\text{Ar}/^{36}\text{Ar})_{\text{AIR}} = 295.5$; $\lambda_e = 0.581 \times 10^{-10} \text{ yr}^{-1}$; analytical uncertainties are $\pm 1\sigma$

Stable Isotope Geochemistry of Alunite

Sulfur

The $\delta^{34}\text{S}$ values of alunites from sediment-hosted micron gold deposits range from 3 to 13 per mil; most are between 7 and 11 per mil (Table 2, Fig. 3). A jarosite analysis from Post has a similar $\delta^{34}\text{S}$ value of 8.6 per mil. These $\delta^{34}\text{S}$ values overlap analyses of primary sulfides from both unaltered Roberts Mountains Formation rocks (diagenetic pyrite: 5–14‰; Rye, 1985) and primary hydrothermal sulfides from sediment-hosted micron gold deposits (Fig. 3). In the weathering environment, primary sulfides are generally converted quantitatively to sulfates by oxidation, with consequent negligible fractionation of sulfur isotopes. Therefore, the sulfur in the sulfates most likely was derived directly from the primary sulfides by weathering (Field, 1966; Ohmoto and Rye, 1979; Bird et al., 1989).

In contrast, barite from alunite-bearing veins at Post and Alligator Ridge (Fig. 2B) is both texturally distinct and is significantly enriched in ^{34}S , with $\delta^{34}\text{S}$ values in excess of 15 per mil. Disseminated and replacement barite at Alligator Ridge is also significantly enriched in ^{34}S relative to alunite (Ilchik, 1990). None of the reported $\delta^{34}\text{S}$ values of barite from Rain or Gold Quarry overlap those of alunite. Therefore, even though these two sulfates may occupy the same vein, alunite and barite have very dif-

TABLE 2. New Stable Isotope Data for Minerals from Sediment-Hosted Micron Gold Deposits

Sample no.	Mineral	Comments	$\delta^{34}\text{S}$	$\delta^{18}\text{O}_{\text{SO}_4}$	$\delta^{18}\text{O}_{\text{OH}}$	δD
118/1230	Pyrite	Post, high-grade altered limestone	1.0			
214/782	Pyrite	Post, endoskarn	-1.0			
3/1154	Pyrite	Post, breccia with pyrite cement	-23.6			
3/1203	Pyrite	Post, breccia with pyrite	-5.0			
241/1783	Pyrite	Post, pyrite-quartz breccia	6.2			
3/1719	Pyrite	Post, diagenetic (?) pyrite	3.7			
ST7/975	Pyrite	Post, fresh Goldstrike stock	7.2			
214/1409	Pyrite	Post, high-grade altered stock	5.6			
214/1412	Pyrite	Post, high-grade altered stock	6.2			
118/1609	Pyrite	Post, altered dike	3.9			
PVS-3	Pyrite	Post, milky quartz-pyrite vein	6.4			
GQ-6	Pyrite	Gold Quarry, pyritic pod in pit	3.9			
67/990	Barite	Post, vuggy vein	13.6	2.4		
241/2022	Barite	Post, vuggy vein in jasperoid	16.0	2.2		
BP-79	Barite	Post, pit alunite-barite vein	26.6	-0.8		
214/1467	Barite	Post, bladed white barite in sediments	31.6	16.8		
118/1757	Barite	Post, massive milky vein	28.9	13.2		
Rossi	Barite	Rossi mine, massive sedex barite	28.0	15.4		
GQ-5220	Barite	Gold Quarry, coarse crystallized blades	38.8	2.4		
GQ-7	Barite	Gold Quarry, clear vuggy crystals	27.9	0.0		
R-8	Barite	Rain, massive pod	29.7	16.7		
R-9	Barite	Rain, euhedral clear	26.5	0.4		
BP-9	Jarosite	Post, pit jarosite	8.6			
BP-79P	Alunite	Post, pit alunite-barite vein	9.2	5.0	3.6	-120
BP-79B	Alunite	Post, brown alunite from pit	11.1	1.2	-1.2	-129
GQ-5280	Alunite	Gold Quarry, massive earthy veins	8.4	-2.8	-7.9	-132
9834A	Alunite	Rain, massive earthy vein	9.0	0.3	-0.4	-159
9835A	Alunite	Rain, replacement pod	10.9	-0.1	0.3	-144
3-2-27	Alunite	Alligator Ridge, fracture fillings		4.5	1.7	-125
197/1102	Kaolinite	Post, in veins with quartz		-0.3		-150
257/1137	Kaolinite	Post, replacement with realgar		1.0		-152
3/830	Kaolinite	Post, white veins		4.2		-147
208/1412	Kaolinite	Post, poddy white in gray sedimentary matrix		-0.6		-147
257/1022	Kaolinite	Post, altered Goldstrike stock		4.9		-155
257/1237	Kaolinite	Post, intermixed with realgar crystals		1.0		-152
267/1499	Kaolinite	Post, contorted light gray lens		5.7		-151
BP-78	Kaolinite	Post, in veins with alunite		10.4		-121
213/1275	Kaolinite	Post, green clay pods in sheared sedimentary matrix		11.6		-139
267/1019	Kaolinite	Post, clay pods in medium gray sedimentary matrix		9.6		-143

Sulfur isotope analyses are reported relative to Canyon Diablo troilite and oxygen and hydrogen isotope analyses are reported relative to SMOW. Uncertainties: $\delta^{34}\text{S} = \pm 0.15\%$; $\delta^{18}\text{O} = \pm 0.2\%$ for kaolinite, $\pm 0.5\%$ for sulfate and hydroxyl; $\delta\text{D} = \pm 2\%$; $\delta^{18}\text{O}$ values reported for kaolinite in the sulfate column are for the entire mineral

ferent sulfur isotope compositions and therefore different origins and different ages. This precludes using the barite-alunite association as an indicator of a hypogene origin for alunite.

Oxygen-hydrogen

Oxygen and hydrogen isotope analyses of alunite from various environments have been summarized by Rye et al. (1991; Fig. 4), who demonstrate that alunite should have distinct isotopic signatures that reflect its origin. Separate analyses of hydroxyl and sulfate oxygen may provide significant insight into the origin of a given specimen, particularly in the case of supergene vs. hypogene alunite. Because of kinetic (disequilibrium) effects, only in supergene alunite can hydroxyl oxygen be enriched in ^{18}O over

sulfate oxygen. In addition, the oxygen and hydrogen isotope composition of cogenetic kaolinite, if present, provides another indication of the origin of the alunite.

Sulfate and hydroxyl from magmatic hydrothermal alunite have δD and $\delta^{18}\text{O}$ values which are close to those of primary magmatic water; sulfate and hydroxyl are in internal equilibrium. Some shifts in both δD and $\delta^{18}\text{O}$ may occur for such alunite due to mixing of magmatic and meteoric waters (Fig. 4). However the amount and direction of that shift is likely to be small while maintaining alunite stability. Steam-heated alunites, which result from the oxidation of gaseous hypogene H_2S by reaction with ground waters in the near-surface environment, have hydrogen isotope compositions slightly depleted in D rela-

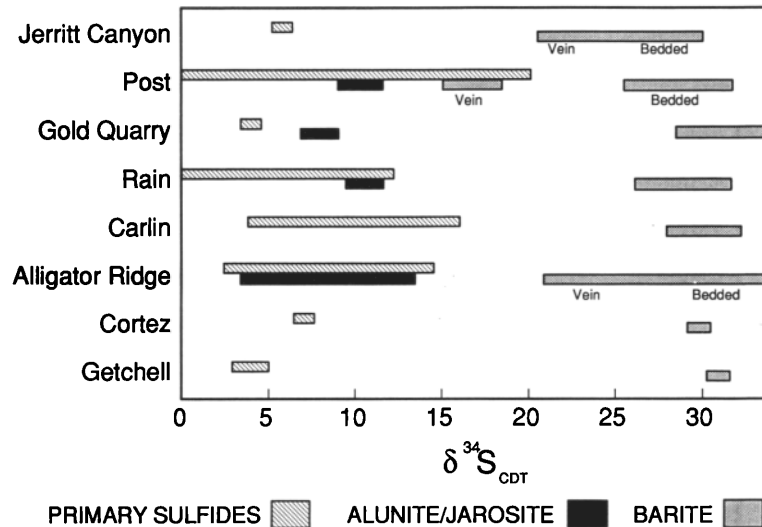


FIG. 3. Compilation of sulfur isotope data of sulfates and sulfides from various sediment-hosted micron gold deposits. At several deposits, a contrast in isotopic signature between bedded and vein barite is recognized. Data from Table 2, Ilchik (1990), Rye et al. (1989), Northrop et al. (1987), Rye (1985), Radtke et al. (1980), and G. B. Arehart, unpub. data.

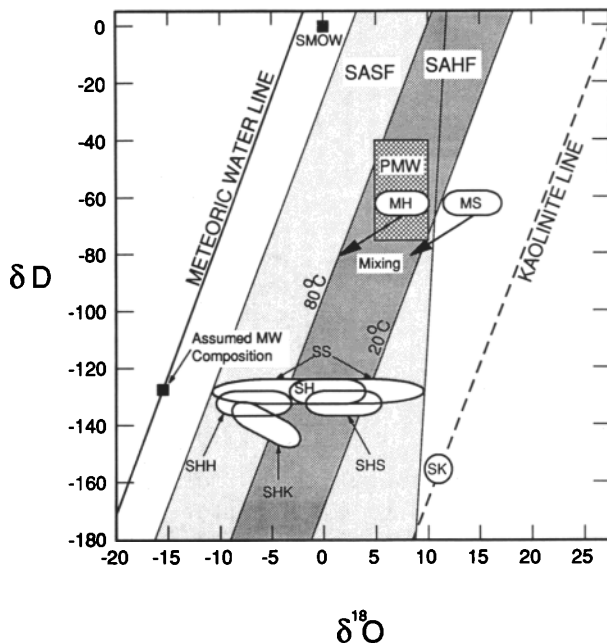


FIG. 4. Generalized systematics of alunitic from various environments, redrawn after Rye et al. (1991). MH = magmatic-related alunitic hydroxyl, MS = magmatic-related sulfate, MW = meteoric water, PMW = primary magmatic water box, SAHF = range of compositions of supergene alunitic sulfate, SH = supergene hydroxyl, SHH = steam-heated hydroxyl, SHK = kaolinite in equilibrium with steam-heated alunitic, SHS = steam-heated sulfate, SK = kaolinite in equilibrium with supergene alunitic, SS = supergene sulfate. Kaolinite line from Savin and Epstein (1970).

tive to water from which they form. Sulfate and hydroxyl oxygen are in internal equilibrium, with sulfate enriched in ^{18}O relative to hydroxyl. Both sulfate and hydroxyl oxygen are enriched in ^{18}O relative to water (Fig. 4), with the degree of enrichment being temperature dependent. Cogenetic kaolinite has $\delta^{18}\text{O}$ values of oxygen which are similar to those of hydroxyl oxygen in alunite; the kaolinite is slightly depleted in D relative to hydroxyl in alunite (Fig. 4).

Bulk analyses of supergene alunitic may encompass a wide range of values (Fig. 4). Sulfate, and consequently bulk oxygen values, may be influenced by both fluid (ground water) and atmospheric oxygen compositions (Rye et al., 1991). Oxygen and hydrogen in hydroxyl of supergene alunite should be in equilibrium with local meteoric water at the time of crystallization and may be used to place constraints on temperature and composition of supergene fluids (Bird et al., 1989; Stoffregen et al., 1989). Therefore separate analyses of sulfate and hydroxyl are desirable.

Oxygen isotope values of hydroxyl from alunite from sediment-hosted micron gold deposits (Table 2, Fig. 5) are all within the supergene alunite hydroxyl zone delineated by Rye et al. (1991). All of these data are consistent with near-surface formation temperatures ($<80^\circ\text{C}$). Sulfate oxygen analyses from the same samples (Table 2, Fig. 5) fall close to hydroxyl values. Temperatures of deposition calculated from these internal fractionations are unrealistically high for alunite stability. This is characteristic of super-

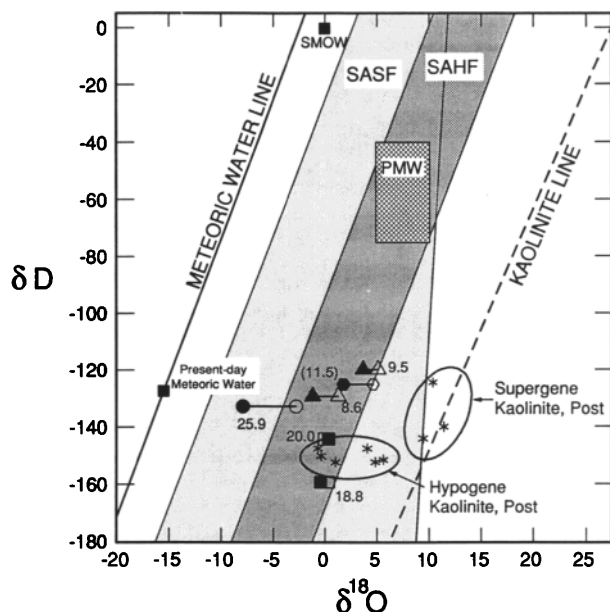


FIG. 5. Oxygen and hydrogen isotope analyses of alunite and kaolinite from various sediment-hosted micron gold deposits plotted on the base of Figure 4. Fields labeled as in Figure 4. Data are from Tables 1 and 2. Triangles = Post samples, squares = Rain samples, circles = Gold Quarry sample, hexagons = Alligator Ridge sample, stars = Post kaolinite samples. Open symbols are sulfate analyses, solid symbols are hydroxyl analyses. Numbers show K/Ar ages for samples. The Alligator Ridge sample (in parentheses) was not dated by us but is probably of similar age to the samples reported by Ilchik (1990).

gene alunite (Pickthorn and O'Neil, 1985) and arises because of kinetic effects preventing attainment of equilibrium.

Data for kaolinite that is cogenetic with alunite from the Post deposit plot on the supergene kaolinite line (Fig. 5). In contrast, hypogene kaolinite formed at higher temperatures, and from a different fluid, has more negative δD and $\delta^{18}O$ values.

Oxygen isotope analyses of barite from several deposits are given in Table 2. The $\delta^{18}O$ values of syndimentary, premineralization barite cluster around 15 per mil, consistent with deposition from Paleozoic seawater. In contrast, $\delta^{18}O$ values of hypogene vein barite have a limited range near 0 per mil. Alunite and barite from the same vein at Post have significantly different sulfate oxygen isotope compositions; the alunite $\delta^{18}O$ value is 5.0 per mil, whereas the barite value is -0.8 per mil, indicating deposition from distinctly different solutions.

There is a clear variation between δD values and age for alunites from these sediment-hosted micron gold deposits (Fig. 5). This relation may reflect a systematic change in the isotopic composition of meteoric water through time in north-central Nevada since 25 Ma (Arehart and O'Neil, 1991). While sev-

eral variables may be responsible for such changes, tectonic arguments effectively rule out significant changes in altitude and latitude. Therefore the observed variation in δD must be reflecting a major climatic change in this region, and perhaps a global one.

Conclusions

Textural and stable isotope evidence and K/Ar ages support the conclusion that alunites in sediment-hosted micron gold deposits are supergene features. These observations agree with other chemical parameters known or inferred for sediment-hosted micron gold alteration and mineralization. Neither field observations at these deposits nor isotopic analyses support a magmatic or steam-heated origin for this alunite. Therefore, alunite is not a useful mineral in the exploration for, or evaluation of, sediment-hosted micron gold deposits. Because of the apparent correlation of age and δD values, such secondary supergene alunite may be a useful mineral in paleoclimatological research. Detailed evaluation of this application is currently in progress (Arehart and O'Neil, 1991).

Acknowledgments

This work was supported by grants from American Barrick Resources, the National Science Foundation (EAR-89-05107), Sigma Xi, and the University of Michigan Turner Fund. The University of Michigan electron microbeam analysis laboratory provided reduced-cost access to facilities to GBA. We thank D. R. Peacor and *Economic Geology* reviewers for insightful reviews of the manuscript.

March 26, November 6, 1991

REFERENCES

- Arehart, G. B., and O'Neil, J. R., 1991, Stable isotope ratios of alunite as an indicator of paleoclimate in continental settings [abs.]: Am. Geophys. Union Chapman Conf. Continental Isotopic Indicators of Climate, Jackson, Wyoming, June, 1991.
- Arehart, G. B., Kesler, S. E., Foland, K. A., and Hubacher, F. A., 1989, Alteration zoning and geochronology of the Post micron gold deposit, Nevada [abs.]: Geol. Soc. America Abstracts with Programs, v. 21, p. A350.
- Ashley, R. P., and Silberman, M. L., 1976, Direct dating of mineralization at Goldfield, Nevada, by potassium-argon and fission-track methods: *ECON. GEOL.*, v. 71, p. 904-924.
- Bagby, W. C., and Berger, B. R., 1985, Geologic characteristics of sediment-hosted, disseminated precious-metal deposits in the western United States: *Rev. Econ. Geology*, v. 2, p. 169-202.
- Bakken, B. M., and Einaudi, M. T., 1986, Spatial and temporal relation between wall rock alteration and gold mineralization, main pit, Carlin gold mine, Nevada, U.S.A., in Macdonald, A. J., ed., *Gold '86: Willowdale, Ontario, Konsult Internat. Inc.*, p. 488-496.
- Bird, M. I., Andrew, A. S., Chivas, A. R., and Lock, D. E., 1989, An isotopic study of surficial alunite in Australia, 1. Hydrogen and sulphur isotopes: *Geochim. et Cosmochim. Acta*, v. 53, p. 3223-3237.
- Bird, M. I., Chivas, A. R., and McDougall, I., 1990, An isotopic study of surficial alunite in Australia, 2. Potassium-argon geochronology: *Geochim. et Cosmochim. Acta*, v. 80, p. 133-145.

- Bonham, H. F., 1985, Characteristics of bulk-mineable gold-silver deposits in cordilleran and island-arc settings: U. S. Geol. Survey Bull. 1646, p. 71-77.
- Chiba, H., Kusakabe, M., Hirano, S., Matsuo, S., and Shigeyuki, S., 1981, Oxygen isotope fractionation factors between anhydrite and water from 100 to 550°C: *Earth Planet. Sci. Letters*, v. 53, p. 55-62.
- Coleman, M. L., Shepherd, T. J., Durham, J. J., Rouse, J. E., and Moore, M. P., 1982, Reduction of water with zinc for hydrogen isotope analysis: *Anal. Chemistry*, v. 54, p. 993-995.
- Cunningham, C. G., Rye, R. O., Steven, T. A., and Mehnert, H. H., 1984, Origins and exploration significance of replacement and vein-type alunite deposits in the Marysvale volcanic field, west-central Utah: *ECON. GEOL.*, v. 79, p. 50-71.
- Field, C. W., 1966, Sulfur isotopic method for discriminating between sulfates of hypogene and supergene origin: *ECON. GEOL.*, v. 61, p. 1428-1435.
- Hayba, D. O., Bethke, P. M., Heald, P., and Foley, N. K., 1986, Geologic, mineralogical, and geochemical characteristics of volcanic-hosted epithermal precious-metal deposits: *Rev. Econ. Geology*, v. 2, p. 129-167.
- Hofstra, A. H., Leventhal, J. S., Northrop, H. R., Landis, G. P., Rye, R. O., Birak, D. J., and Dahl, A. R., 1990, Genesis of sediment-hosted disseminated-gold deposits by fluid mixing and sulfidization: Chemical-reaction-path modeling of ore-depositional processes documented in the Jerritt Canyon district, Nevada: *Geology*, v. 19, p. 36-40.
- Ilchik, R. P., 1990, Geology and geochemistry of the Vantage gold deposits, Alligator Ridge-Bald Mountain mining district, Nevada: *ECON. GEOL.*, v. 85, p. 50-75.
- Jewell, P. W., and Parry, W. T., 1987, Geology and hydrothermal alteration of the Mercur gold deposit, Utah: *ECON. GEOL.*, v. 82, p. 1958-1966.
- Kuehn, C. A., and Rose, A. W., 1987, Chemical and mineralogical zonation associated with low pH hydrothermal alteration at the Carlin gold deposit, Nevada [abs.]: *Geol. Soc. America Abstracts with Programs*, v. 19, p. 734.
- Lloyd, R. M., 1968, Oxygen isotope behavior in the sulfate-water system: *Jour. Geophys. Research*, v. 73, p. 6099-6110.
- Naeser, C. W., 1979, Fission-track dating and geologic annealing of fission tracks, in Jager, E., and Hunziker, J. C., *Lectures in isotope geology*: Berlin, Springer-Verlag, p. 154-169.
- Northrop, H. R., Rye, R. O., Landis, G. P., Lustwerk, R., and Daly, W. E., 1987, Sediment-hosted disseminated gold mineralization at Jerritt Canyon, Nevada. V—Stable isotope geochemistry and a model of ore deposition [abs.]: *Geol. Soc. America Abstracts with Programs*, v. 19, p. 791.
- Ohmoto, H., and Rye, R. O., 1979, Isotopes of sulfur and carbon, in Barnes, H. L., ed., *Geochemistry of hydrothermal ore deposits*: New York, Wiley Intersci., p. 509-567.
- Pickthorn, W., and O'Neil, J. R., 1985, ^{18}O relations in alunite minerals: Potential single-mineral geothermometer [abs.]: *Geol. Soc. America Abstracts with Programs*, v. 17, p. 689.
- Radtke, A. S., 1985, Geology of the Carlin gold deposit, Nevada: U. S. Geol. Survey Prof. Paper 1267, 124 p.
- Radtke, A. S., Rye, R. O., and Dickson, F. W., 1980, Geology and stable isotope studies of the Carlin gold deposit, Nevada: *ECON. GEOL.*, v. 75, p. 641-672.
- Robinson, B. W., and Kusakabe, M., 1975, Quantitative preparation of sulfur dioxide, for $^{34}\text{S}/^{32}\text{S}$ analyses, from sulfides by combustion with cuprous oxide: *Anal. Chemistry*, v. 47, p. 1179-1181.
- Rye, R. O., 1985, A model for the formation of carbonate-hosted disseminated gold deposits based on geologic, fluid inclusion, geochemical, and stable isotope studies of the Carlin and Cortez deposits, Nevada: U. S. Geol. Survey Bull. 1646, p. 35-42.
- Rye, R. O., Bethke, P. M., and Wasserman, M. D., 1989, Diverse origins of alunite and acid-sulfate alteration: Stable isotope systematics: U. S. Geol. Survey Open-File Rept. 89-5, 33 p.
- 1991, The stable isotope geochemistry of acid-sulfate alteration and vein forming alunite: U. S. Geol. Survey Open-File Rept. 91-257, 59 p.
- Savin, S. M., and Epstein, S., 1970, The oxygen and hydrogen isotope geochemistry of clay minerals: *Geochim. et Cosmochim. Acta*, v. 34, p. 25-42.
- Sharp, Z. D., 1990, A laser-based microanalytical method for the in situ determination of oxygen isotope ratios of silicates and oxides: *Geochim. et Cosmochim. Acta*, v. 54, p. 1353-1358.
- Stoffregen, R. E., Rye, R. O., and Wasserman, D. M., 1989, Experimental determination of ^{18}O (sulfate site) and D fractionations between alunite and water at 250 to 450°C [abs.]: *Geol. Soc. America Abstracts with Programs*, v. 21, p. A155.
- Tooker, E. W., 1985, Discussion of the disseminated-gold-ore-occurrence model: U. S. Geol. Survey Bull. 1646, p. 107-150.
- Wells, J. D., and Mullens, T. E., 1973, Gold-bearing arsenian pyrite determined by microprobe analysis, Cortez and Carlin gold mines, Nevada: *ECON. GEOL.*, v. 68, p. 187-201.